Author's Accepted Manuscript

www.elsevier.com/locate/talanta

A microfluidic platform with pneumatically switchable single-cell traps for selective intracellular signals probing

Yao Wang, Jinchi Zhu, Peng Chen, Liang Hu, Xiaojun Feng, Wei Du, Bi-Feng Liu

PII: S0039-9140(18)31003-8
DOI: https://doi.org/10.1016/j.talanta.2018.09.085
Reference: TAL19099

To appear in: *Talanta*

Received date: 8 June 2018
Revised date: 12 September 2018
Accepted date: 23 September 2018

Cite this article as: Yao Wang, Jinchi Zhu, Peng Chen, Liang Hu, Xiaojun Feng, Wei Du and Bi-Feng Liu, A microfluidic platform with pneumatically switchable single-cell traps for selective intracellular signals probing, *Talanta,* https://doi.org/10.1016/j.talanta.2018.09.085

A microfluidic platform with pneumatically switchable single-cell traps for selective intracellular signals probing

Yao Wang[a,b,1], Jinchi Zhu[a,1], Peng Chen[a], Liang Hu[a], Xiaojun Feng[a], Wei Du[a,*], Bi-Feng Liu[a]

[a]Britton Chance Center for Biomedical Photonics at Wuhan National Laboratory for Optoelectronics-Hubei Bioinformatics & Molecular Imaging Key Laboratory, Systems Biology Theme, Department of Biomedical Engineering, College of Life Science and Technology, Huazhong University of Science and Technology, Wuhan 430074, China

[b]Wuhan Centers for Disease Prevention and Control, Wuhan, 430074, China

[*]Corresponding author: College of Life Science and Technology, Huazhong University of Science and Technology, Wuhan 430074, China, Tel: +86-27-87792203; fax: +86-27-8779217, weidu@mail.hust.edu.cn

Abstract

To investigate rapid suspension cell signaling, a microfluidic platform was urgently needed for flexibly manipulation of single cells and simultaneous generation of controllable chemical signals to stimulate single cells. In this paper, a microfluidic biosensor was developed to monitor intracellular calcium signal, integrated with single-cell trapping, chemical stimulation and releasing. Selective entrapment and discharge of individual cell were achieved by controlling the deformable membrane with pneumatic traps. The activation of intracellular calcium signal was qualitatively and quantitatively investigated by high-controllable chemical single-cell stimulation based on flexible hydrodynamic gating. And performing chemical stimulation and control assay in the same channel would improve the experimental robustness and effectiveness. Further investigation of the cellular responses to ATP pulses of varying concentrations and durations indicated that 20 μM ATP pulses with duration as short as 200 ms resulted in the same level of Ca^{2+} response induced by sustained stimulations. Washing with buffer for 30 s was sufficient for single cell to recover from receptor desensitization caused by ATP stimulation. In addition, the responses of cells to ATP stimulation were heterogeneous. The developed microfluidic method opens up a new avenue for intracellular signaling studies and drug screening.

[1] These authors contributed equally to this work

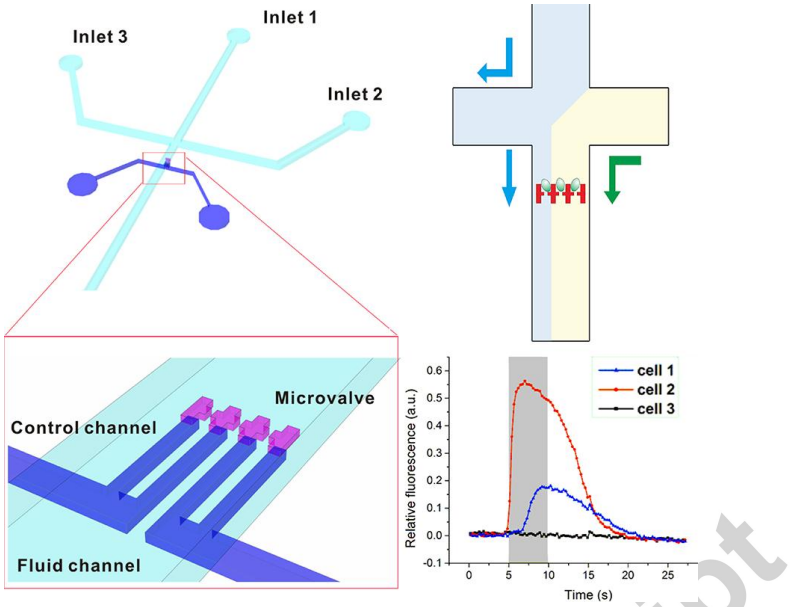

Keywords: microfluidic biosensor; pneumatic valve; single-cell trapping; hydrodynamic gating; intracellular calcium signal

1. Introduction

Many critical cellular decisions, such as apoptosis, cell cycle checkpoints, and cytoskeletal reorganization are very sensitive to temporal and spatial dynamics of extracellular microenvironments [1]. Some environmental factors involved in these cellular decisions include chemical signals, such as cytokines, nutrients, growth factors, and hormones, biological signals originating from cell-contact processes, and physical signals, including mechanical (shear stress, cytoskeletal tension, stretch-activated ion channels), electrical (voltage-gated ion channels, gal-vanotaxis), and thermal (temperature-sensitive ion channels, biochemical kinetics) factors [2]. Currently, localized environmental stimulations are widely used to study receptor-mediated intracellular calcium signaling [3-10]. Compare with mechanical and electrical stimulations, chemical stimulations provide a more physiological input to cells [11]. However, the generation of fast-changing and accurate chemical stimulation to cells is still an enormous challenge using traditional methods based on micro-perfusion.

The emerging microfabrication and microfluidics technology are now allowed to improve the precision and reliability of controlling environmental variables for single-cell analysis. These technological platforms combining systems analysis of signaling pathways are expected to guide an improved quantitative description of the function of individual cells [12-16]. For example, Lu group has been committed to investigate cellular signals by using dynamic stimulation profiles based on microfluidic chips [17-20]. Previously, several microfluidic devices were proposed for on-chip monitoring intracellular calcium signal with high temporal and spatial resolution in our

group [21-23]. However, the focal point in these research was all aim to adherent cells, lacking the ability to manipulate suspension cells. For a long time, time-lapse functional imaging of suspension cells was technically challenging, because of the movement of target cells during stimulation and imaging. In response to an increasing demand for cell positioning, various microfluidic techniques, such as optical tweezers methods [24], micropipettes methods [25], microwell-based platforms [26,27], dielectrophoresis-based systems [28-30] and hydrodynamic-based systems [31-36], have been developed to capture cells, retain them in a specific location. Among them, microwells and hydrodynamic-based microfluidic platforms using the passive capturing mechanism could realize precise cell position and dynamical stimulation. However, these platforms were often difficult to capture targeted cells selectively and further release the trapped cells. In contrast, other platforms based on the positive capturing mechanism (optical tweezers, micropipettes, dielectrophoresis) were harmful to the cells and difficult to dynamically chemically stimulate the cells during the manipulation of cell positioning.

Combining the superiority of flexible cell manipulation and dynamically cell stimulation, a novel semi-automated microfluidic cell-based biosensor was proposed to monitor intracellular calcium signal. The micro-device was composed of fluid channels, pneumatic valves relied on deformable membrane, and control channels. The pneumatic valves were used for trapping of single cells and timely release of the trapped cell. The custom-designed LabView™ program was used to manipulate the platform for multiple single-cell analysis. Selective chemical stimulation to the trapped single-cell was achieved by a hydrodynamic gating technique for inducing the intracellular signals. For proof of principle, intracellular calcium signal of suspended cells under dynamic stimulation of ATP was qualitatively and quantitatively investigated by using this micro-device.

2. Material and methods

2.1. Chemicals and reagents

Chemicals such as NaCl, KCl, $CaCl_2$, $MgCl_2$, HCl, NaOH, fluorescein, and D-glucose were purchased from Sinopharm Chemical Reagent (Shanghai, China). Adenosine 5'- triphosphate disodium salt ($ATPNa_2$), 4-(2-hydroxyethyl)-1-piperazineethanesulfonic acid (HEPES), penicillin, streptomycin，and dimethyl sulfoxide (DMSO) were purchased from Sigma-Aldrich (St. Louis, MO). Tyrode's solution containing 137 $mmolL^{-1}$ NaCl, 5.4 $mmolL^{-1}$ KCl, 1.0 $mmolL^{-1}$ $MgCl_2$, 1.3 $mmolL^{-1}$ $CaCl_2$, 10 $mmolL^{-1}$ D-glucose, and 10 $mmolL^{-1}$ HEPES (pH adjusted to 7.2 using NaOH) as the buffer solution. Fluorescein was prepared in the buffer solution at a final concentration of 2×10^{-6} $molL^{-1}$. Fluo-3/AM (Biotium, Hayward, CA) stock solution (2.0 $mmolL^{-1}$) in DMSO was diluted in buffer solutions at a final concentration of 10 $\mu molL^{-1}$. $ATPNa_2$ was dissolved in the buffer solution at a final concentration of 10 $\mu molL^{-1}$ as the agonist. All reagents were of analytical grade unless noted otherwise. All solutions were prepared with water purified by the Direct-Q system (Millipore, Bedford, MA) and filtered with 0.22 μm sterilized syringe filters prior to use.

Instrumentation.

A custom-built pressure control system was based on the published protocol [21, 37], which contained a microfluidic chip, four independent E/P transducers, a solenoid valve and a

LabView™-based signal control module. The pressures of the fluid were precisely controlled by four independent E/P transducers (T-1001, Bellofram, USA). The E/P transducer could reduce a supply pressures (compressed nitrogen cylinder) to a regulated output pressure directly proportional to a three-wire voltage input with 0.1% accuracy. The pneumatic traps were controlled by the off-chip solenoid valve (VDW250-5G-2-01, SMC, Japan). All the operated E/P transducers and solenoid valve were controlled by a PCI controller card (NI6703, National Instruments, Austin, TX) and a custom-designed LabView™ program.

Experiments were performed on an inverted fluorescence microscope (IX71, Olympus, Japan) with a CCD camera (Evolve 512, photometrics, USA) for image acquisition. Excitation beam from a mercury lamp was first filtered by a 460- to 490-nm band-pass excitation filter, reflected off a 505-nm dichroic mirror and then focused on the microchannel by a 60×objective (NA 0.7) or a 40× objective (NA 0.6). Fluorescent signals were collected through the same objective, filtered using a 510-nm high-pass filter and finally monitored by a CCD camera. Finally, acquired images were further analyzed using image pro plus 6.0, and origin 7.5.

2.2. Micro-device fabrication

The microfluidic device was fabricated by a rapid prototyping method [38] and based on the well-established "PDMS flow-control layer" technique [39,40]. Microfluidic channels were designed by a CAD program (AutoCAD 2014, Autodesk, USA) and printed on a transparent film as photomasks (3000 dpi film, Shanghai). The micro-device was assembled with three layers: a fluid layer, a middle PDMS membrane and a control layer (Fig. 1). The fluid layer had a crossed-channel architecture, and typical channels were 250 μm wide and 20 μm high. The pneumatic traps in the PDMS membrane were used for the entrapment of individual cells, which were 50 μm high. The control layer was 30 μm high. SU-8™ (GM1070, Gersteltec Sarl, Switzerland) mold was fabricated on 3-inch silicon wafers using standard soft-lithography technique. The PDMS, made from a mixture of base oligomers and curing agent in a mass ratio of 10:1, were fabricated by molding the SU-8 structure. Specially, the middle thin PDMS membrane was fabricated by spin-coating PDMS prepolymer on a silicon wafer at 700 rpm for 60 s followed by incubation at 95 ℃ for 1 h. Then, the PDMS sheet was cut and peeled off from the mold. The two layers and the thin membrane were treated with oxygen plasma treatment for 2 min (PDC-GC-M, Weike Spectrum, China), aligned and brought together to form an irreversible seal.

2.3. Cell culture and preparation

NIH-3T3 and HeLa cells were purchased from the American Type Culture Collection (ATCC, Manassas, VA). The cells were maintained by passaging twice weekly with Dubelcco's Modified Eagle Medium (DMEM) supplemented with 10% fetal bovine serum (FBS), 100 μg/mL penicillin, and 100 μg/mL streptomycin. Cells were maintained in a 37 ℃ incubator with 5% CO_2-humidified air atmosphere and passaged every 2 or 3 days. For loading, adherent cells were detached from 100 mm diameter culture dishes with 2 mL trypsin EDTA (0.25%, Gibco, Carlsbad, CA). An equal amount of DMEM + FBS was then added to deactivate remaining trypsin. Cells were then centrifuged to a pellet and resuspended in phosphate buffered saline pH 7.4 (PBS, Gibco, Carlsbad, CA). Cultures were maintained between 1.0×10^5 and 1.0×10^7 cells/ml. Serial

dilutions were performed with supplemented DMEM.

2.4. Procedure of microchip operation

Before cell loading, the microchip was treated with oxygen plasma, added with 75 % ethanol and incubated in a clean bench at room temperature for 30 min. The microchannel was then washed with buffer solution and cell culture media, sequentially. Fig. 2 shows a schematic illustration of the procedure for operating the microchip. The inlet was loaded with 100 μl NIH-3T3 cells (1×10^6/mL) while the outlet was kept empty. Cells were introduced into the microfluidic channel with the hydrostatic pressures. Positive pressure was then applied to deform the membrane, so the suspension cells were trapped. Renewing the media in the inlet to wash redundant cells. Then, chemical stimulation was achieved by microfluidic gated flow. Finally, switching the pneumatic trap to close, meanwhile, the cells were released. This micro-device was recyclable, and could perform cell stimulation experiment multiple times. Add PBS to the inlet to wash the microchip, then the cell stimulation experiment could be conducted again.

2.5. Calcium imaging

Cells trapped by microvalves were washed gently with tyrode's solution and then incubated with 10 μM fluo-3/AM at 37 ℃ for 30 min via gravity-driven perfusion. Then, tyrode's solution was loaded into the fluid channels to replace Fluo-3/AM. The microchannels and reservoirs were filled with tyrode's solutions at 37 ℃ for 10 min. Once gated-flow solution of agonist was pumped into the fluid channel for stimulating cells locally, fluorescent images were captured by a CCD (Evolve 512, Photometrics, USA) at 200 ms interval with an exposure time of 200 ms.

3. Results and discussion

3.1. Characterization of the membrane deformation

We employed a push-up PDMS membrane to capture single cell. PDMS membrane is flexible and readily deforms into a curvature, leading to decreased distance between the bottom of fluid channel and PDMS membrane. When the distance decreases to a smaller size than individual cells, cell entrapment by pneumatic micro-valves could be performed.

To investigate the membrane deformation under different pressures, fluorescein (0.1 mg ml^{-1}) was injected into the microfluidic device. When the gas pressure was increased, fluorescein solution was pushed out from the middle channel by the deformed membrane so that the fluorescence intensity was decreased at pneumatic micro-valves. Therefore, the membrane deformation could be reflected by the intensity of fluorescein in the middle channel. As shown in Fig. 3, the fluorescence intensity under 0.4 MPa and 0.5 MPa were similar, indicating the pneumatic micro-valves had been saturated when the pressure reach 0.4 MPa.

3.2. Trapping individual cells by membrane deformation

The procedure for trapping individual cells was as follows: while the pneumatic micro-valves

were closed, 50 μL of cells (1×10^5 mL^{-1}) were loaded into inlet 1, inlet 2, inlet 3, and the outlet was kept empty. Cells were allowed to flow into the downstream channels. Then, the pneumatic micro-valves were actuated, the push-up PDMS membrane was moderately deformed by applying 0.4 MPa pressure in the control layer. The height of the flow channel decreased at the compressive area. The cell would be captured by the compressive valve traps once flowing through this area (Fig. 4). When left valve or right valve was open respectively, only one cell could be trapped in the compressive valve traps. When left valve and right valve were open simultaneously, three individual cells could be trapped in the compressive valve traps. This resulted from the design of the particular trapping structures in the PDMS membrane. Two middle cross-shaped fences could make up a new single-cell capture structure when two set of micro-valves were simultaneously actuated. After chemical stimulation and recording of trapped single-cell, two micro-valves were close simultaneously, three single cells could be released. For multiple single-cell analysis, positive pressure was again applied to deform the membrane of micro-valves for trapping another single suspended cells.

3.3. Evaluation of single-cell stimulation

The flow visualization experiments were first applied to validate the feasibility of the pinched-flow microchip, which could provide guidance for further investigation of ATP stimulation. Because of the similarity between the diffusion constant of fluorescein (500 μm^2 s^{-1}) and ATP (360 μm^2 s^{-1}), we used 1×10^{-7} mol L^{-1} fluorescein solution to visualize the flow patterns and to reveal the relationship between the pressure distribution and the position of the pinched-flow.

According to the published protocol, the change of pressures at inlet 1and inlet 2 can change the proportion of stimuli solution in the cell trapping channel [24]. In our experiments, the pressure at inlet 1 was fixed at a constant value. The pressure at inlet 2 was varied to change the laminar flow interface for single-cell stimulation by switching the gating states between stimulation OFF and stimulation ON. Figure 5 illustrated the fluorescence distribution across the cell trapping channel at ~250 μm downstream of the intersection under different pressures. As the pressure at inlet 2 changed from 1.0 to 1.8 kPa, the width of fluorescein flow (defined as a distance from the microchannel wall to where fluorescence intensity drops to 10 % of the maximum value) decreased linearly (R^2=0.999, Fig. 5c). Furthermore, we calculated that the mean lateral diffusion distance (defined as a distance over which the fluorescence intensity of fluorescein flow drops from 90% to 10% of the maximum value) of the stimulation solution was limited to ~10 μm.

3.4. Calcium signals in single suspended cells

NIH-3T3 cells expressing endogenous ATP receptors were employed as the sensing element. According to the results of flow visualization experiment, we further applied the pinched-flow to stimulate the single NIH-3T3 cells with ATP solution. Fluo-3 was used as the intracellular calcium indicator for investigating the developed single-cell biosensor.

Since the shear stress may induce calcium transients in endothelial cells, we evaluated the effect of shear stress on $[Ca^{2+}]_i$ by exposing the cells to pulses of buffer solutions. As a result, the

$[Ca^{2+}]_i$ remained constant, suggesting that the abrupt change of shear stress did not account for calcium spikes during hydrodynamic gated sample injection in our proposed micro-device (Fig. 7a).

Previous literature showed that NIH-3T3 cells respond to ATP at the concentrations from 1 to 100 μM in a dose-dependent manner [41]. Here, after trapping three single cells, ATP solution of 10 μM was pinched to stimulate the target cell for 5 s with 2 min intervals for studying ATP-induced intracellular Ca^{2+} spike in single cells. According to the position of target cell 1 in the channel (Fig. 6a) and the profile of pinched-flow (Fig. 5), the pressure at inlet 2 was chosen as 1.3 kPa to stimulate only cell 1. With localized stimulation of ATP for 5 s, cell 1 showed a quick increase of $[Ca^{2+}]_i$, un-stimulated cell 2 and cell 3 had no change of $[Ca^{2+}]_i$ (Fig. 6d). For the stimulation of cell 1 and 2, the pressure at inlet 2 was chosen as 1.5 kPa. With localized stimulation of ATP for 5 s, cell 1 and cell 2 showed a quick increase of $[Ca^{2+}]_i$, cell 3 had no change of $[Ca^{2+}]_i$ (Fig. 6b and e). When the pressure at inlet 2 was 1.7 kPa, cell 2 and cell 3 both showed a quick increase of $[Ca^{2+}]_{i\ with}$, cell 1 showed a slow increase of $[Ca^{2+}]_i$. After stimulation of ATP solution, the amplitude of calcium spikes decreased gradually due to receptor desensitization (Fig. 6c and f). These results suggested that this micro-device could achieve the chemical stimulation of single suspended cells by the pinched-flow. In addition, the chemical stimulation and control experiments could be performed simultaneously in the same channel, which significantly improved the robustness and effectiveness of the assay.

3.5. Calcium signals under multiple stimulations

Thus, we further investigated intracellular calcium signals in individual cells under multiple stimulations with different conditions. Pulses of 20 μM ATP were first used to repetitively simulate the trapped single-cell as chemical environment factor. When 20 μM ATP of 200 ms duration were introduced with 30 s intervals, the amplitude of calcium spikes of single NIH-3T3 cell maintained at a similar level (Fig. 7b). The results suggested that the 30 s interval was sufficient for NIH-3T3 cells to recover from the ATP-receptors desensitization induced by 200 ms stimulations.

To further investigate the cellular responses to ATP pulses with different durations from millisecond to second in this platform, 20 μM pulses of ATP with increasing durations of 200 ms, 1 s, 4 s, 8 s and 10 s were applied to the same single cell. Fig. 7c showed that the amplitude of Ca^{2+} spike increased gradually as the duration increased from 200 ms to 4 s. The amplitude of Ca^{2+} spike with durations of 8 s, 10 s obviously decreased. In addition, the decay time of Ca^{2+} spike (defined as a time for $[Ca^{2+}]_i$ decline) increased gradually with the increasing duration from 200 ms to 10 s.

To test the sensitivity of the single suspended cell to ATP in this microfluidic platform, 200 ms pulses of ATP with increasing concentrations of 1 μM, 10 μM, 100 μM and 1 mM were injected to stimulate cells. Significant increases of $[Ca^{2+}]_i$ in response to 1 μM ATP were observed (Fig. 7d), indicating a high sensitivity of this micro-device as single-cell based biosensor for detecting ATP. And the amplitude of Ca^{2+} spike maintained at a similar level in response to 10 μM, 100 μM and 1 mM ATP.

4. Conclusions

The microfluidic biosensor was developed to monitor intracellular calcium signal, integrated with cell trapping, chemical stimulation and cell releasing. Capturing and liberating individual cell was achieved by controlling the PDMS membrane with gas valves. In contrast to unalterable trapping structures, pneumatic traps could be switched between open and close status under the control of a computer, which make the micro-device for multiple single-cell analysis based on chemical stimulation and cell recording. Intracellular calcium signal was activated by high-controllable chemical stimulation based on the gated pinched-flow. Performing single-cell chemical stimulation and control assay simultaneously in the same channel significantly improved the experimental robustness and effectiveness. The micro-device was used to qualitatively and quantitatively investigate the single-cell intracellular calcium responses to ATP pulses with different durations from millisecond to second and different concentrations. In addition, other functionalities, including high-throughput management of single cell and chemical stimulation by microfluidic hydrodynamic gated as well as the exchange of reagents, can be readily integrated in one microfluidic chip for real-time investigating Ca^{2+} signaling in the future. This developed microfluidic method opens a new avenue for intracellular signaling studies and drug screening.

Conflict of interest

The authors declare that there is no conflict of interest relating to this work.

Acknowledgements

We gratefully acknowledge the financial supports from National Natural Science Foundation of China (21775049, 21475049, 31471257 and 31700746) and National Key R&D Program of China (2016YFF0100801), and the China Postdoctoral Science Foundation funded project (2018M630847 and 2018T110753), and the General Program of Health and Family Planning Commission of Hubei Province of China (WJ2017M198).

References

[1] B.L. Hogan, Morphogenesis, Cell 96(2) (1999) 225-33.

[2] D. Di Carlo, L.P. Lee, Dynamic single-cell analysis for quantitative biology, Anal. Chem. 78(23) (2006) 7918-25.

[3] B.M. Gumbiner, Regulation of cadherin-mediated adhesion in morphogenesis, Nat. Rev. Mol. Cell Biol. 6(8) (2005) 622-34.

[4] A. Rustom, R. Saffrich, I. Markovic, P. Walther, H.H. Gerdes, Nanotubular highways for intercellular organelle transport, Science 303(5660) (2004) 1007-10.

[5] B. Geiger, A. Bershadsky, Exploring the neighborhood: adhesion-coupled cell mechanosensors, Cell 110(2) (2002) 139-42.

[6] C.A. Ahern, R. Horn, Stirring up controversy with a voltage sensor paddle, Trends Neurosci. 27(6) (2004) 303-7.

[7] M.E. Mycielska, M.B. Djamgoz, Cellular mechanisms of direct-current electric field effects: galvanotaxis and metastatic disease, J. Cell Sci. 117(Pt 9) (2004) 1631-9.

[8] H. Lee, M.J. Caterina, TRPV channels as thermosensory receptors in epithelial cells, Pflugers Arch. 451(1) (2005) 160-7.

[9] E.M. Lucchetta, J.H. Lee, L.A. Fu, N.H. Patel, R.F. Ismagilov, Dynamics of Drosophila embryonic patterning network perturbed in space and time using microfluidics, Nature 434(7037) (2005) 1134-8.

[10] D.E. Jaalouk, J. Lammerding, Mechanotransduction gone awry, Nat. Rev. Mol. Cell Biol. 10(1) (2009) 63-73.

[11] S. Zibek, B. Hagmeyer, A. Stett, M. Stelzle, Chemical stimulation of adherent cells by localized application of acetylcholine from a microfluidic system, Front Neuroeng. 3 (2010) 113.

[12] P.J. Lee, T.A. Gaige, P.J. Hung, Dynamic cell culture: a microfluidic function generator for live cell microscopy, Lab Chip 9(1) (2009) 164-6.

[13] X.Y. Zhang, M.G. Roper, Microfluidic Perfusion System for Automated Delivery of Temporal Gradients to Islets of Langerhans, Anal. Chem. 81(3) (2009) 1162-1168.

[14] K. Takeda, D. Shao, M. Adler, P.G. Charest, W.F. Loomis, H. Levine, A. Groisman, W.J. Rappel, R.A. Firtel, Incoherent feedforward control governs adaptation of activated ras in a eukaryotic chemotaxis pathway, Sci. Signal. 5(205) (2012) ra2.

[15] R.A. Kellogg, S. Tay, Noise facilitates transcriptional control under dynamic inputs, Cell 160(3) (2015) 381-92.

[16] M.G. Roper, Cellular Analysis Using Microfluidics, Anal. Chem. 88(1) (2016) 381-394.

[17] K. Chung, C.A. Rivet, M.L. Kemp, H. Lu, Imaging single-cell signaling dynamics with a deterministic high-density single-cell trap array, Anal. Chem. 83(18) (2011) 7044-52.

[18] L. Chingozha, M. Zhan, C. Zhu, H. Lu, A generalizable, tunable microfluidic platform for delivering fast temporally varying chemical signals to probe single-cell response dynamics, Anal. Chem. 86(20) (2014) 10138-47.

[19] L. He, A. Kniss, A. San-Miguel, T. Rouse, M.L. Kemp, H. Lu, An automated programmable platform enabling multiplex dynamic stimuli delivery and cellular response monitoring for high-throughput suspension single-cell signaling studies, Lab Chip 15(6) (2015) 1497-507.

[20] A.S. Kniss-James, C.A. Rivet, L. Chingozha, H. Lu, M.L. Kemp, Single-cell resolution of intracellular T cell Ca2+ dynamics in response to frequency-based H2O2 stimulation, Integr. Biol. 9(3) (2017) 238-247.

[21] P. Chen, Y. Guo, X. Feng, S. Yan, J. Wang, Y. Li, W. Du, B.F. Liu, Microfluidic Chemical Function Generator for Probing Dynamic Cell Signaling, Anal. Chem. 89(17) (2017) 9209-9217.

[22] J. Sun, J. Wang, P. Chen, X. Feng, W. Du, B.F. Liu, A chemical signal generator for resolving temporal dynamics of single cells, Anal. Bioanal. Chem. 400(9) (2011) 2973-81.

[23] J. Sun, P. Chen, X. Feng, W. Du, B.F. Liu, Development of a microfluidic cell-based biosensor integrating a millisecond chemical pulse generator, Biosens. Bioelectron. 26(8) (2011) 3413-9.

[24] Z. Lu, C. Moraes, G. Ye, C.A. Simmons, Y. Sun, Single cell deposition and patterning with a robotic system, PloS One 5(10) (2010) e13542.

[25] J. Tang, R. Peng, J. Ding, The regulation of stem cell differentiation by cell-cell contact on micropatterned material surfaces, Biomaterials 31(9) (2010) 2470-6.

[26] J. Doh, M. Kim, M.F. Krummel, Cell-laden microwells for the study of multicellularity in lymphocyte fate decisions, Biomaterials 31(12) (2010) 3422-8.

[27] J.R. Rettig, A. Folch, Large-Scale Single-Cell Trapping and Imaging Using Microwell Arrays, Anal. Chem. 77(17) (2005) 5628-5634.

[28] J. Voldman, M.L. Gray, M. Toner, M.A. Schmidt, A microfabrication-based dynamic array cytometer, Anal. Chem. 74(16) (2002) 3984-90.

[29] D.S. Gray, J.L. Tan, J. Voldman, C.S. Chen, Dielectrophoretic registration of living cells to a microelectrode array, Biosens. Bioelectron. 19(7) (2004) 771-80.

[30] R.S. Thomas, H. Morgan, N.G. Green, Negative DEP traps for single cell immobilisation, Lab Chip 9(11) (2009) 1534-40.

[31] D. Di Carlo, N. Aghdam, L.P. Lee, Single-cell enzyme concentrations, kinetics, and inhibition analysis using high-density hydrodynamic cell isolation arrays, Anal. Chem. 78(14) (2006) 4925-30.

[32] A.M. Skelley, O. Kirak, H. Suh, R. Jaenisch, J. Voldman, Microfluidic control of cell pairing and fusion, Nat. Methods 6(2) (2009) 147-52.

[33] J.P. Frimat, M. Becker, Y.Y. Chiang, U. Marggraf, D. Janasek, J.G. Hengstler, J. Franzke, J. West, A microfluidic array with cellular valving for single cell co-culture, Lab Chip 11(2) (2011) 231-7.

[34] X. Han, Z. Liu, L. Zhao, F. Wang, Y. Yu, J. Yang, R. Chen, L. Qin, Microfluidic Cell Deformability Assay for Rapid and Efficient Kinase Screening with the CRISPR-Cas9 System, Angew. Chem. Int. Edit. 55(30) (2016) 8561-5.

[35] K. Zhang, C.K. Chou, X. Xia, M.C. Hung, L. Qin, Block-Cell-Printing for live single-cell printing, Proc. Natl. Acad. Sci. U. S. A. 111(8) (2014) 2948-53.

[36] Y. Li, J. H. Jang, C. Wang, B. He, K. Zhang, P. Zhang, T. Vu, and L. Qin, Microfluidics Cell Loading-Dock System: Ordered Cellular Array for Dynamic Lymphocyte-Communication Study, Adv. Biosys. 1 (2017) 1700085.

[37] L. Hu, A. Ge, X. Wang, S. Wang, Y. Gao, X. Feng, W. Du, B.F. Liu, An on-demand gas segmented flow generator with high spatiotemporal resolution for in vivo analysis of neuronal response in C. elegans, Lab Chip 16(20) (2016) 4020-4027.

[38] D.C. Duffy, J.C. McDonald, O.J. Schueller, G.M. Whitesides, Rapid Prototyping of Microfluidic Systems in Poly(dimethylsiloxane), Anal. Chem. 70(23) (1998) 4974-84.

[39] M.A. Unger, H.P. Chou, T. Thorsen, A. Scherer, S.R. Quake, Monolithic microfabricated valves and pumps by multilayer soft lithography, Science 288(5463) (2000) 113-6.

[40] T. Xu, W. Yue, C.W. Li, X. Yao, M. Yang, Microfluidics study of intracellular calcium response to mechanical stimulation on single suspension cells, Lab Chip 13(6) (2013) 1060-9.

[41] S. Giovannardi, C. Racca, L. Bertollini, E. Sturani, A. Peres, P2Y purinoceptors in normal NIH 3T3 and in NIH 3T3 overexpressing c-ras, Exp. Cell Res. 202(2) (1992) 398-404.

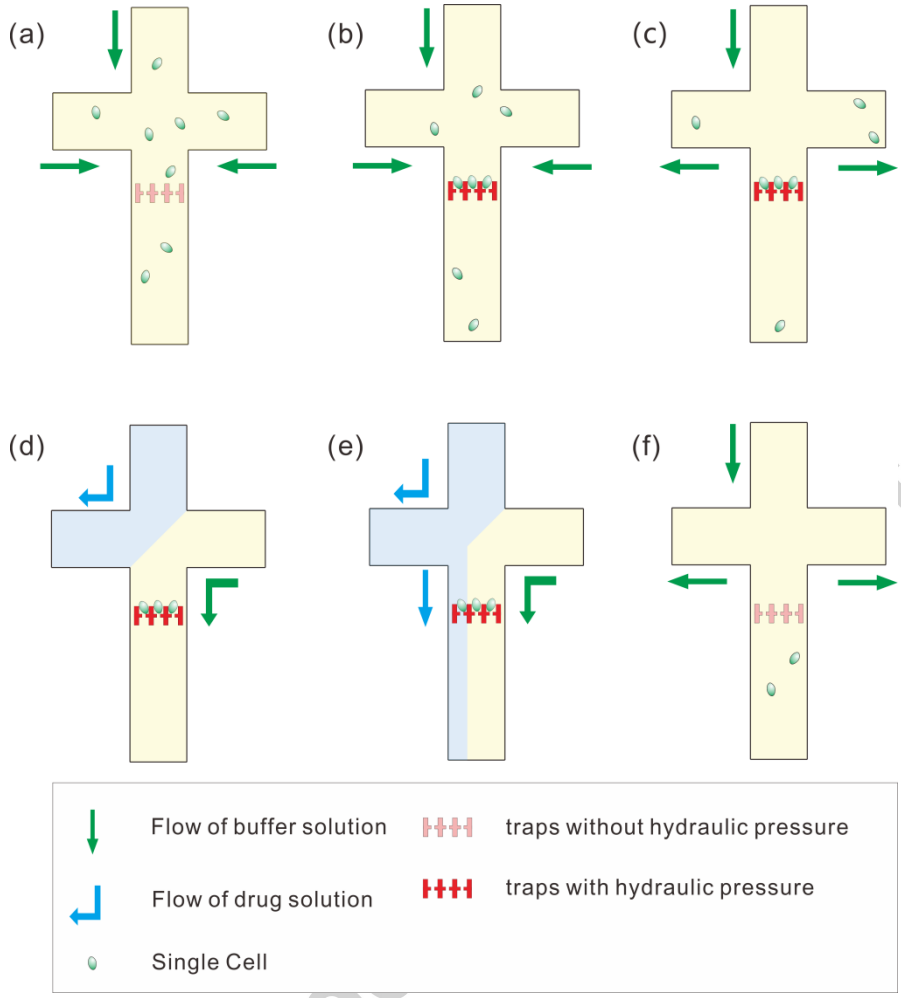

Figure 1. Platform illustrations. (a) Schematic diagram of the microfluidic chip. A deformable PDMS membrane (red) was sandwiched between a fluid layer (green) and a control layer (blue). (b) Micrograph of the micro-device. The scale bar is 200 μm. (c) Schematic diagram of the sub-unit for cell trapping containing the micro-valves, the fluid channel and the control channel. (d) The assembly of the micro-device based on "PDMS flow-control layer" technique. (e) Graphic representation of cell trapping with micro-valves controlled by hydraulic pressure.

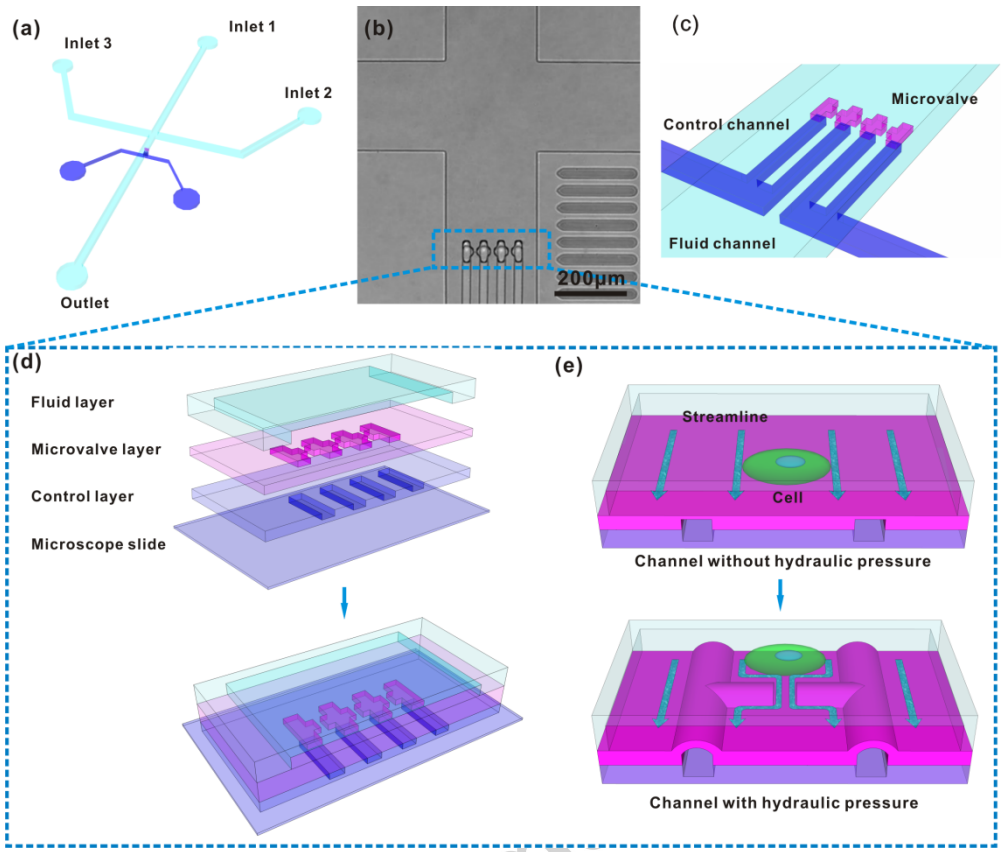

Figure 2. Trap-and-release mechanism and experimental setup. (a) While the pneumatic valves were closed, cells were loaded. (b) The pneumatic valves were actuated, so cells were captured. (c) Buffer was used to washed away residual cells. (d, e) Stimulation of the cells by using chemical reagent. (f) The micro-valves were closed, and cells were wash away. Then the micro-device could be recycled.

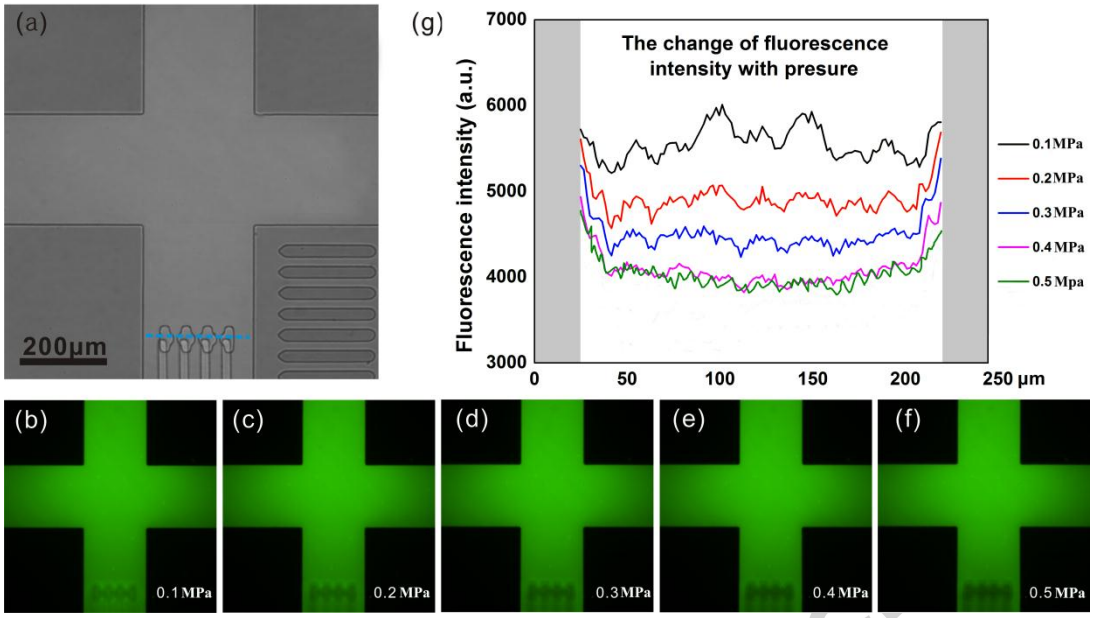

Figure 3. Fluorescence intensities reflected the degree of the membrane deformation. (a) The PDMS membrane was covered by the fluid channel (bright field). The fluorescence intensity change was recorded along the blue dash line. (b)-(f) The fluorescence of fluorescein in the fluid channel from 0.1 to 0.5 MPa, respectively. (g) The change of fluorescence intensity with pressure, ranging from 0.1 to 0.5 MPa.

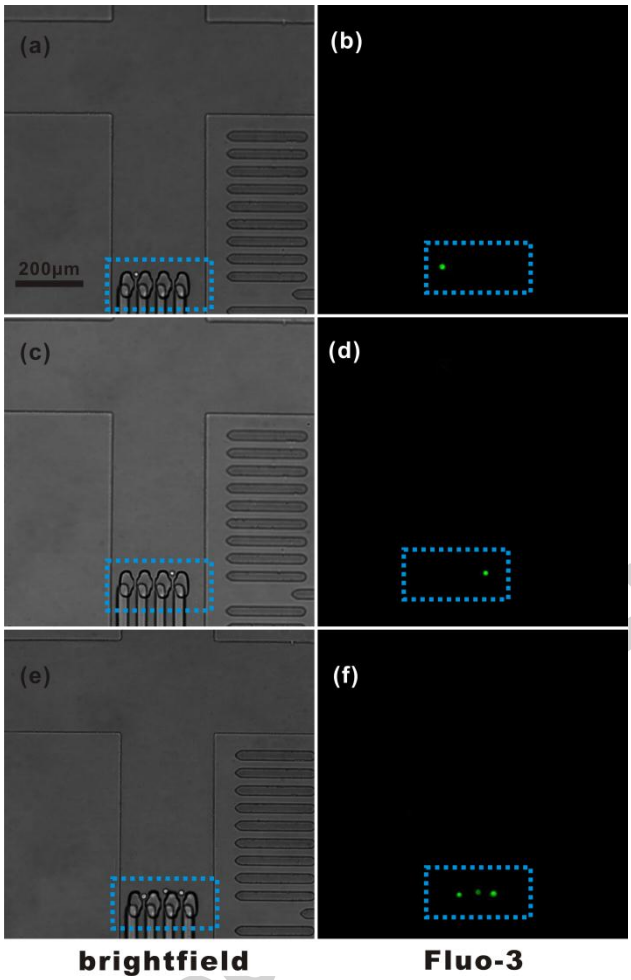

Figure 4. Micrographs of the entrapment of individual 3T3 cells in the fluid channel. After loaded fluo-3, 3T3 cells were introduced into the microfluidic channel. One single cell could be trapped when only the left (a, b) or right (c, d) micro-valve was on, respectively; Three individual cells could be trapped when the two micro-valves (e, f) were on, simultaneously.

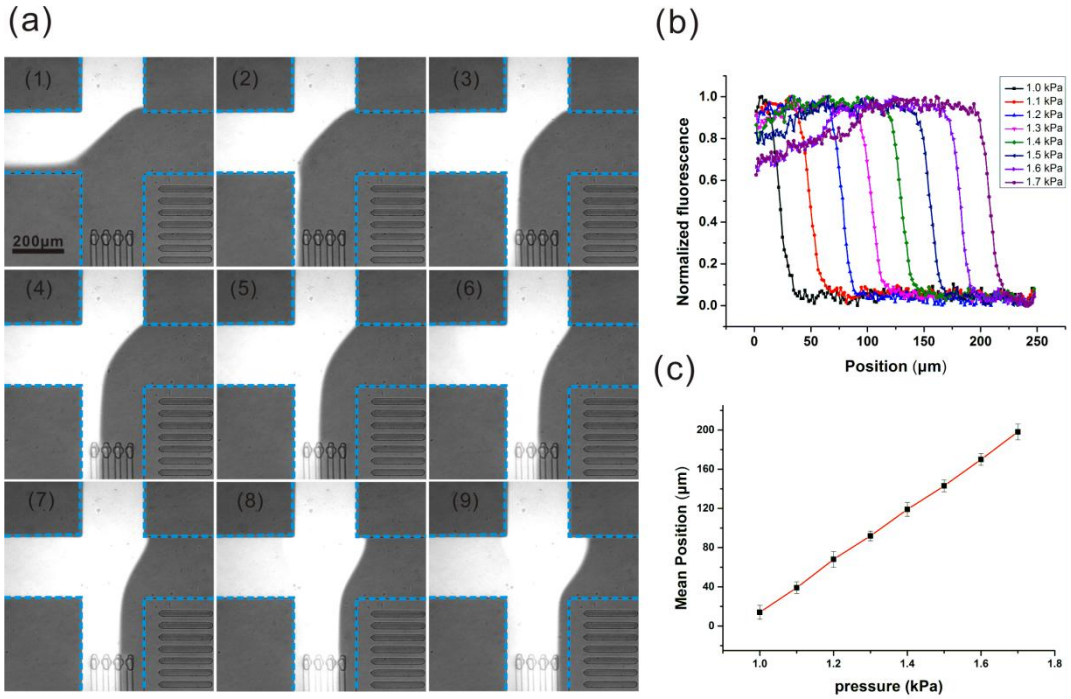

Figure 5. visualization experiments. (a) Visualization experimental diagram of different injecting factor. (b) The fluorescence distribution across the channel ~250 μm downstream of the intersection at different pressures. (c) The quantitative analysis of fluorescence distribution across the channel at different pressures. Error bar indicated standard deviation of three experiments, R^2=0.999.

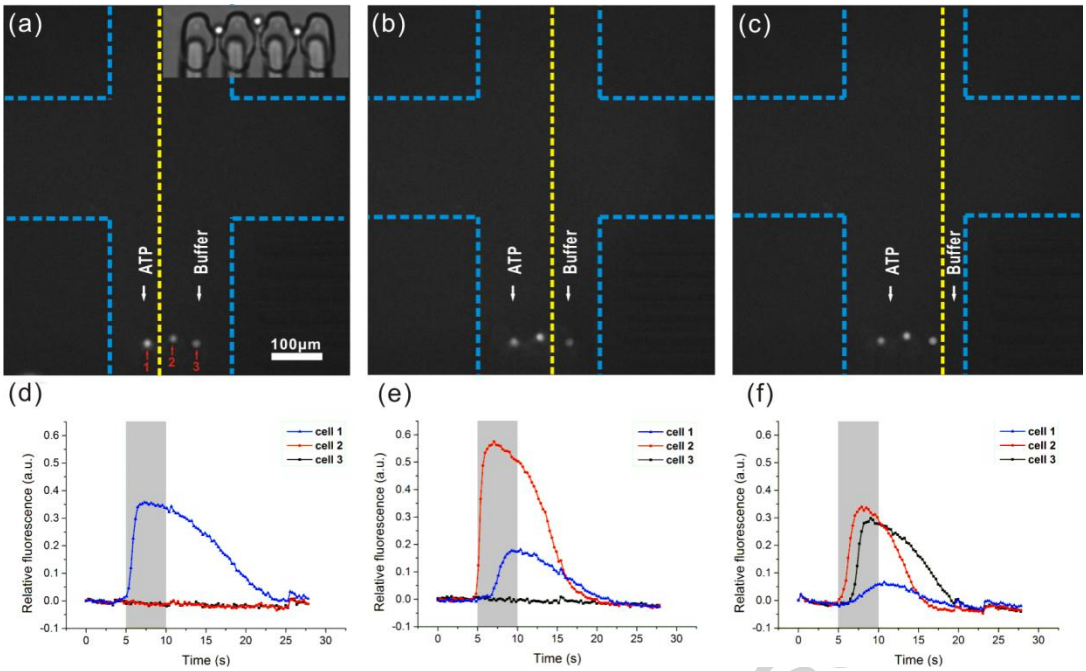

Figure 6. Single cellular chemical stimulation by microfluidic gated flow. (a-c) Intracellular calcium signals under localized ATP stimulation to cell 1, 2, 3 by gated flow at different pressures. (d-f) Time course of the fluorescence intensity of fluo-3 loaded NIH-3T3 cells in (a-c).

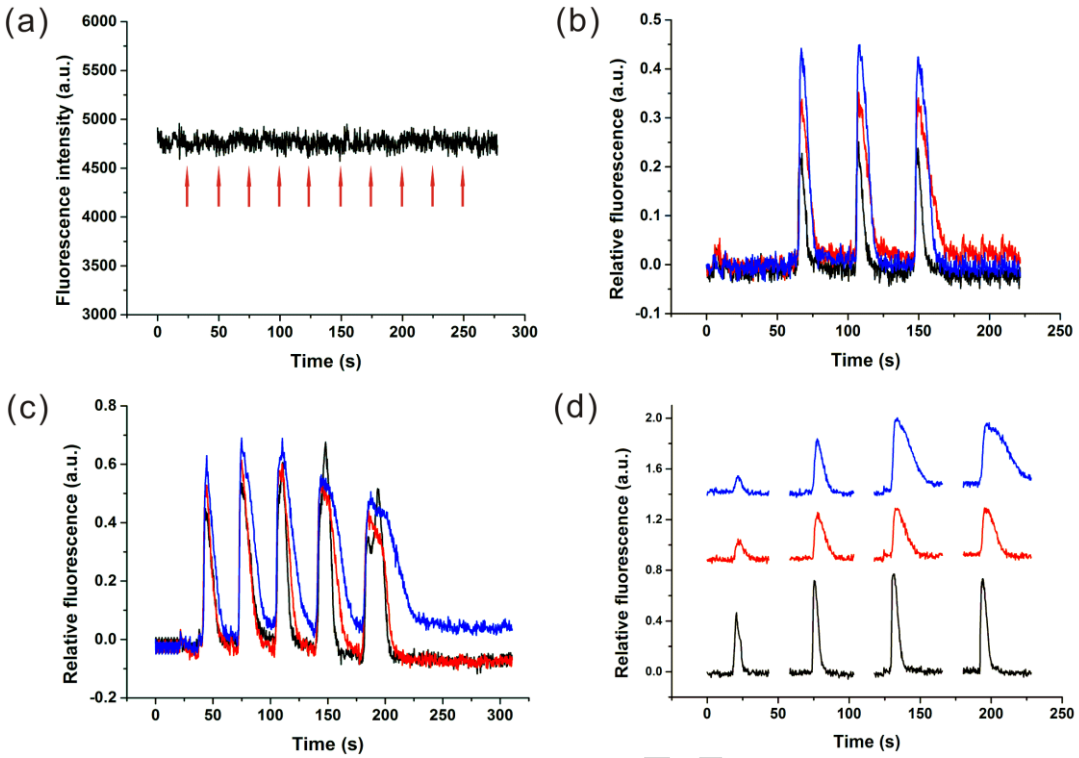

Figure 7. Evaluation of the micro-device with different chemical stimulations. (a) Typical intracellular Ca^{2+} responses to the pulses of buffer solutions. (b) Typical intracellular Ca^{2+} responses to repetitive pulses of 20 μM ATP with 200 ms duration and 30 s intervals. (c) Typical intracellular Ca^{2+} responses to 20 μM ATP pulses of 200 ms, 1 s, 4 s, 8 s and 10 s with 30 s intervals, successively. (d) Typical intracellular Ca^{2+} responses to 200 ms pulses of 1 μM, 10 μM, 100 μM, 1 mM ATP, successively. Three color represent three different single cells.

Highlights

- We presented a semi-automated microchip for single-cell intracellular signals analysis.
- A controllable pneumatic trap was used to trap and discharge suspended cell with single-cell precision.
- The chemical stimulation to cell was achieved by flexible hydrodynamic gating, with highly temporal and spatial resolution.